

PAPER • OPEN ACCESS

Multi-physics Simulation of Heat Transfer in Pulse Electrochemical Machining (PECM) Process

To cite this article: M Fang *et al* 2019 *IOP Conf. Ser.: Mater. Sci. Eng.* **592** 012079

View the [article online](#) for updates and enhancements.



IOP | ebooks™

Bringing you innovative digital publishing with leading voices to create your essential collection of books in STEM research.

Start exploring the collection - download the first chapter of every title for free.

Multi-physics Simulation of Heat Transfer in Pulse Electrochemical Machining (PECM) Process

M Fang^{1,*}, T S Sun¹, Y S Su¹ and Y L Chen²

¹ School of Mechanical and Automotive Engineering, Anhui Polytechnic University, Wuhu 241000, China

² School of Mechanical Engineering, Hefei University of Technology, Hefei 230009, China

* Corresponding Author: fangming@ahpu.edu.cn

Abstract. A multi-physics model is presented for numerical simulation of temperature evolution during quasi steady state (QSS) in pulse electrochemical machining (PECM) process. A fluid model consisting of wall-model and Reynolds-averaged Navier-Stokes equations is used for solving low-Re electrolyte flow near the wall and turbulent flow of electrolyte in the middle channel. A method that the boundary conditions and bulk sources are averaged in time is introduced to make the time-steps not dictated by the time scale of the pulses and SS calculations cheap. The influence of reaction heat sources, joule heat source and inlet flow rate on temperature evolution has been investigated. Simulation results indicate that the influence of reaction heat source on electrode temperature is greater than the electrolyte and most of the joule heat is carried away by the electrolyte flow.

1. Introduction

Similar to DC electrochemical machining, pulse electrochemical machining (PECM) is based on the mechanism of anodic dissolution to remove metal. Therefore, PECM can be used in machining of difficult-to-cut metallic material, in which a high quality surface can be obtained, as well as tool wear and influence of thermal or mechanical on the workpiece are avoided [1]. Due to the application of current or voltage pulses, PECM can reach the more desired surface quality and machining precision, which is primarily attributed to smaller gap sizes, improved anodic polarization process which reduces the material dissolution at low current density regions [2], and improved electrolyte flow [3].

However, in PECM, for the time scale of the applied pulses is orders of magnitude smaller than the time scale of temperature conduction in the electrodes, simulation of the temperature evolution would be a computationally very expensive process. Time accurate calculations of the temperature distribution in PECM process have already been performed to solve the problem by Kozak [4-6], where the assumption was made that a single pulse is valid over a series of pulses and the influence of the electrodes on the temperature distribution in electrolyte was neglected. Smets, et al. [7] calculated temperature transients with thin electrode of 3mm high. To calculate temperature evolution with the higher electrode, a time averaged temperature calculations method was introduced by Smets, et al. [8-10], making the assumption that the electrode is always at a uniform temperature.

In this paper, a multi-physics model is established to describe mathematically ECM process by coupling electric field, flow field and temperature field. To efficiently calculate the temperature distribution in the Quasi Steady State (QSS), the Quasi Steady State ShortCut (QSSSC) approach [8] is



introduced to solve the problem of multi-time scale in PECM process. A wall-model combined with Reynolds-averaged Navier-Stokes equations is introduced to precisely and efficiently solve temperature evolution near the electrolyte-electrode interfaces. A full understanding of the effect of these interactions on temperature evolution is vital for practical applications and for real electrode shape change under PECM conditions.

2. Multi-physical model

Figure 1 shows that a 2D geometric model containing the numbering of boundaries and sample points in PECM process. The cathode and the anode are respectively at the top and the bottom, between which electrolyte is pumped from left to right. The length of the anode and the cathode are both 45 mm. The height is of the anode and the cathode are respectively 29 mm and 60 mm.

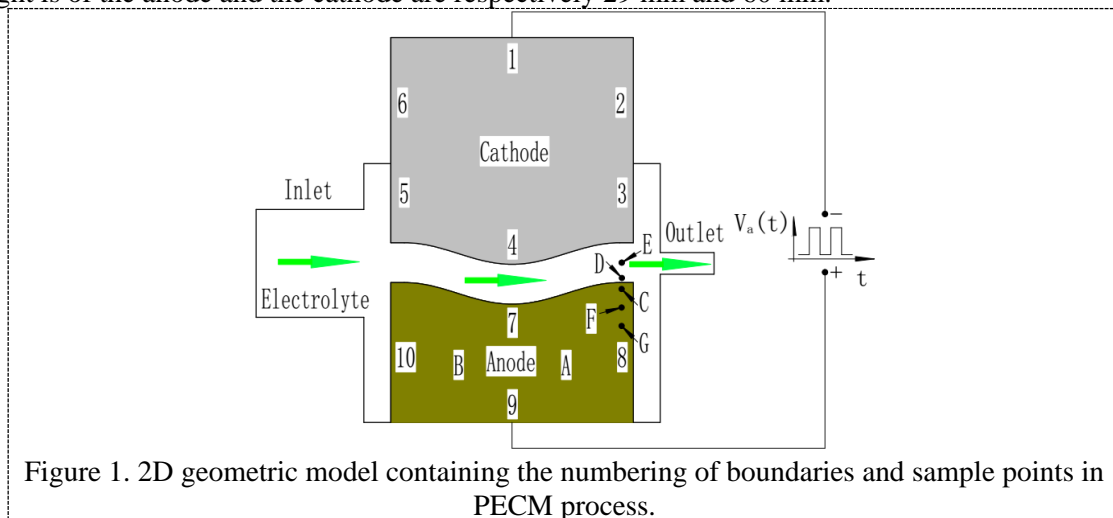


Figure 1. 2D geometric model containing the numbering of boundaries and sample points in PECM process.

2.1. Electrical model

Assuming that the electrode's conductivity σ_1 is constant, the potential V in the electrodes is given by the law of charge conservation:

$$\nabla \cdot (\sigma_1 \nabla V) = 0 \quad (1)$$

The solution for the potential U in the electrolyte is obtained by expressing charge conservation:

$$\nabla \cdot (\sigma \nabla U) = 0 \quad (2)$$

For the electrolyte electrical conductivity σ , a linear model for temperature dependence is introduced [11]:

$$\sigma = \sigma_{\text{ref}} [1 + \gamma(T - T_{\text{ref}})] \quad (3)$$

where, γ is temperature dependence coefficient, taken 0.02 K^{-1} and σ_{ref} is the electrolyte electrical conductivity at the reference temperature T_{ref} .

At the electrolyte-cathode interface Γ_4 and the electrolyte-anode interface Γ_7 , the polarization behavior is represented by a linearized temperature dependent model [12]:

$$j_k = [1 + \alpha(T - T_{\text{ref}})] \frac{V - U - Q_k}{R_k} \quad (4)$$

where, α is a constant introduced to determine the magnitude of temperature dependence, taken 0.02 K^{-1} , j_k is the reaction current density, R_k is the polarization resistance and Q_k is the onset of polarization.

Γ_1 on the cathode is connected with ground and set to zero, and Γ_8 on the anode is set to $V_a(t)$. The other sidewalls are considered electrically insulated.

2.2. Fluid model

In PECM process, turbulence of the electrolyte can effectively flush away the electrolyte in the gap. Therefore, the transient, incompressible Reynolds-averaged Navier-Stokes (RANS) equations are used as follows:

$$\begin{cases} \rho \frac{\partial \mathbf{v}}{\partial t} + \rho(\mathbf{v} \cdot \nabla)\mathbf{v} = \nabla \cdot \left[-p + (\mu + \mu_T)(\nabla\mathbf{v} + (\nabla\mathbf{v})^T) \right] \\ \rho \nabla \cdot (\mathbf{v}) = 0 \end{cases} \quad (5)$$

with \mathbf{v} the electrolyte velocity, ρ the electrolyte density, p the Pressure, μ the dynamic viscosity and μ_T the turbulent viscosity coefficient.

Assuming transient incompressible flow without buoyancy, the model solves the following transport equations for k and ϵ . However, in near-wall area, the electrolyte can't reach the turbulence state. So a wall-function method is introduced to solve the electrolyte flow in near-wall area [12].

2.3. Thermal model

Because of the very high conductivity, joule heating in the electrodes can be negligible. The transient distribution of temperature in the electrode is calculated by the internal energy balance as follow:

$$\rho C_p \frac{\partial T}{\partial t} = \nabla \cdot (K \nabla T) \quad (6)$$

where, C_p is the specific heat capacity and K is the thermal conductivity of the electrode material.

At the interfaces, the reaction heat is taken away by forced convection of electrolyte and is conducted into the electrodes. The reaction heat is imposed as:

$$P_k^{dl} = \eta_k j_k \quad (7)$$

where, η_k is the overpotential.

The temperature evolution in the electrolyte is described by convection-diffusion equation with joule heat source as follow [13]:

$$\rho C_p \frac{\partial T}{\partial t} + \rho C_p \mathbf{v} \nabla T = \nabla \cdot (K \nabla T) + P_{bulk} \quad (8)$$

where, P_{bulk} is the joule heat.

3. Simulation method and parameters

3.1. Simulation method

The influence relation of multi-physical fields on temperature field is shown as Figure 2. When PECM process reaches the QSS, the movement speed of the cathode is almost equal to the rate of anode dissolution. Therefore, the assumption that geometry structure is fixed can be made. For the influence of temperature on kinematic viscosity is little, it is considered that flow field is only affected by import and export pressure. However, electric field is affected by electrolytic conductivity which is associated with temperature distribution in the gap and has a significant influence on temperature field via reaction heat and joule heat.

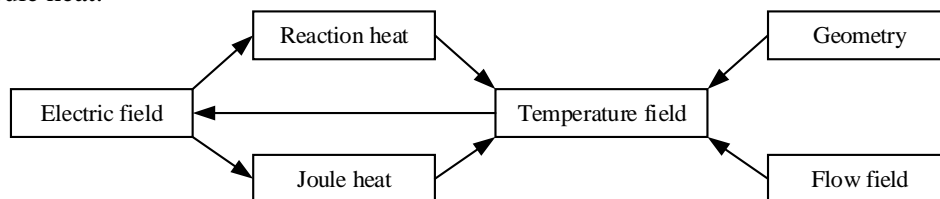


Figure 2. The influence relations of multi-physical fields.

In PECM process, the time scale of heat conduction in the electrodes is orders of magnitude larger than the time scale of heat convection in the electrolyte. A method that the boundary conditions and bulk

sources are averaged in time is introduced to make the time-steps not dictated by the time scale of the pulses and SS calculations cheap. The time averaging operator $\langle \cdot \rangle$ can be defined as [8]:

$$\langle \varphi(t) \rangle = \frac{1}{\tau} \int_t^{t+\tau} \varphi(\lambda) d\lambda \quad (9)$$

3.2. Simulation parameters

The following parameters were used for all simulations (unless stated otherwise). The pulse voltage amplitude and pulse period were respectively 15 V and 20 ms. The duty cycle was 20%. The inlet mass flow rate was 4 kg/s and the work gap was 0.3 mm. The reference temperature was 293.15 K. The physical parameters used in the simulation for the electrolyte and electrodes could be found in Table 1. The polarization parameters for the electrode reactions are shown in [14].

Table 1. Physical parameters of the electrodes and electrolyte

	σ (S/m)	ρC_p (J/m ³ K)	K (W/mK)
Electrolyte	7.2	4.17×10^6	0.58
Electrodes	1.25×10^6	3.56×10^6	25

The whole geometry was discretized into a computational mesh of about 3608 quadrilateral elements and about 52700 triangular elements. The geometry mesh and zooming mesh in the middle of channel are presented in Figure 3.

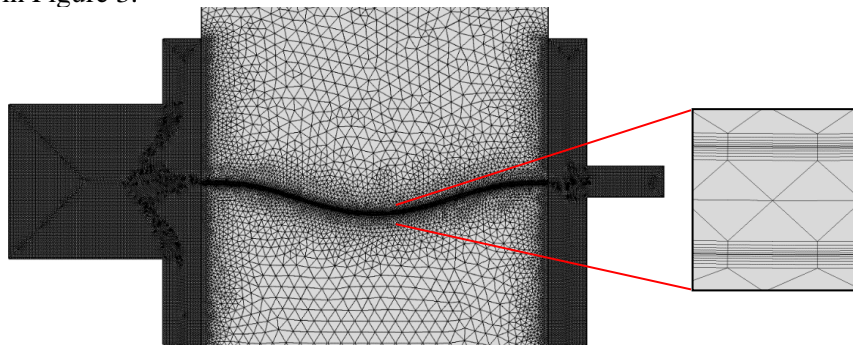


Figure 3. Geometry configuration and mesh.

4. Results and discussion

4.1. Influence of reaction heat sources

Joule heat in the electrolyte is neglected to better reflect the effect of reaction heat in the simulation. The time scale for electrode heat transfer is much larger than the time scale of pulse period. Therefore, to study the influence of reaction heat sources on QSS temperature distribution and make computation cheap, SS of the system is used as the initial state before calculating the QSS.

The reference points C and D near the electrolyte-electrode interface are respectively located in the electrode and electrolyte (See Figure 1). With current pulses applied, the temperature evolutions at reference points C and D are obtained, as shown in Figure 4. The temperature in the electrodes is larger than in the electrolyte. When the value of the critical upper limit Ψ is set as 9×10^{-3} K, the QSS is reached after applying six pulses. Figure 5 presents the variations of the heat flux transferred into the electrodes and electrolyte during one period in QSS. Most of the reaction heat generated in the double layer goes to heat the electrode surface and about 16% of the reaction heat leaves the system by electrolyte flow during the pulse on-time. However, the heat in the electrode is transferred into the electrolyte during the off-time.

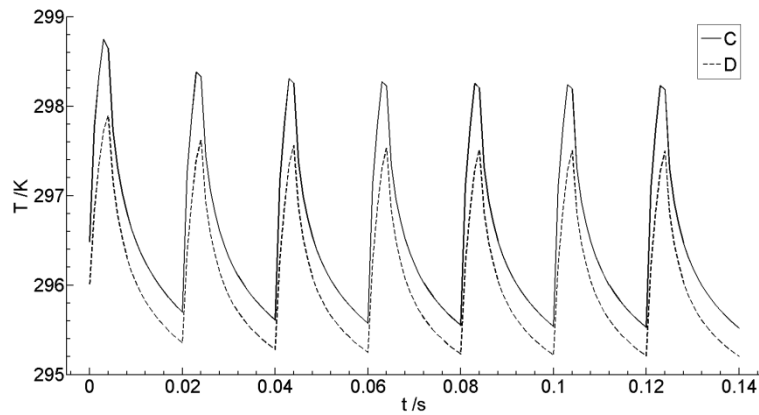


Figure 4. Temperature evolutions at reference points C and D.

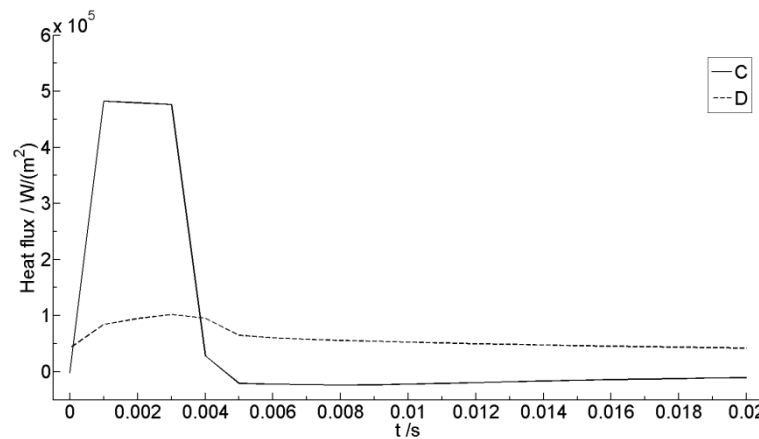


Figure 5. Variations of heat flux at reference points C and D.

4.2. Influence of joule heat source

To study the influence of joule heat source on QSS temperature distribution, reaction heat sources are neglected. Figure 6 presents the temperature evolution at reference points C, D and E (See Figure 1). The pulsating amplitude and the peak of temperature at the point E are largest.

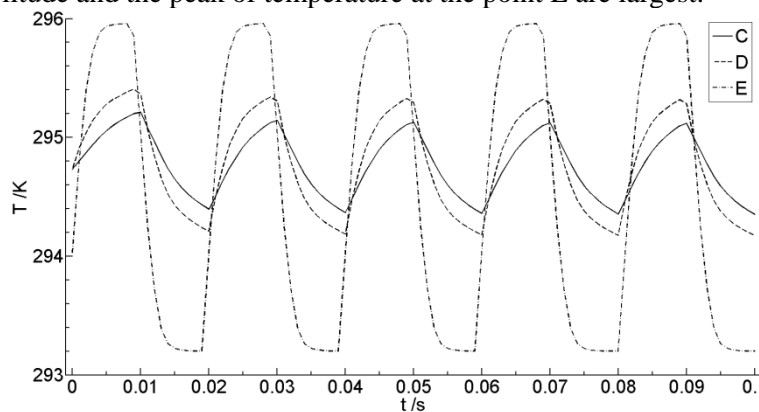


Figure 6. The temperature evolution at reference points C, D and E.

In the electrodes, the temperature evolution at reference points C, F and G are shown in Figure 7. The closer to the electrolyte-electrode interfaces, the larger the pulsating amplitude of temperature is and the shorter the delaying time reaching the peak of temperature is. The delaying time is caused by the time scale of heat conduction in the electrodes.

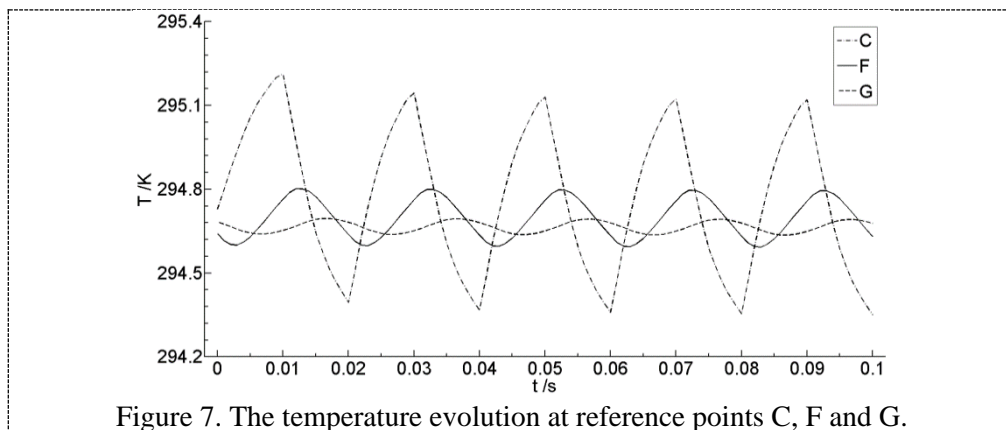


Figure 7. The temperature evolution at reference points C, F and G.

4.3. Influence of the inlet flow rate

The duty cycle was set as 30%. The inlet mass flow rates respectively were 2 kg/s, 3 kg/s and 4 kg/s. And other parameters were used, as shown in section 3.2. The influence of the electrolyte velocity on the temperature evolution was discussed.

Temperature evolution along the vertical channel direction with different inlet flow rates at 5 ms and at the end in one period during QSS near the outlet of channel are presented in Figure 8 and Figure 9. Temperature at the anode-electrolyte interface is largest, which is due to the influence of reaction heat source. Moreover, the anode is immersed into electrolyte, the upside of cathode is in contact with air and the size of cathode is higher than the anode (See Figure 1), which results in the higher temperature in the anode.

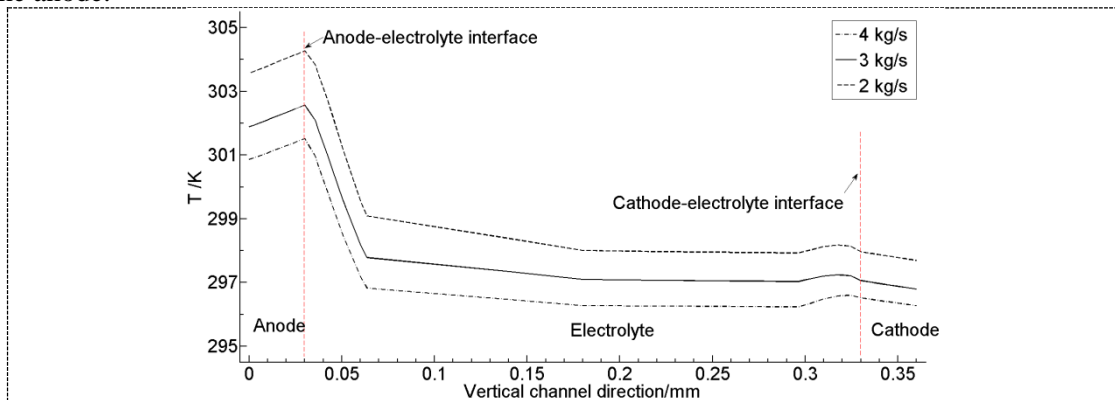


Figure 8. Temperature evolution along the vertical channel direction at 5 ms.

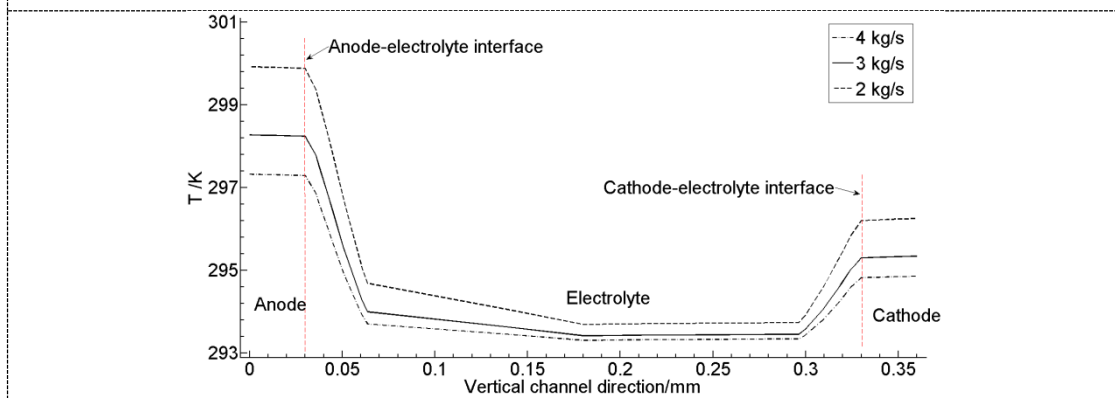


Figure 9. Temperature evolution along the vertical channel direction at the end

During the off-time, the electrolyte is replenished and the heat is flushed away in the channel. When the inlet flow rates are 4 kg/s and 3 kg/s, both of the electrolyte temperature in the middle channel are very close to the reference temperature at the end of the period. But when the inlet flow rate is 2 kg/s, the electrolyte temperature is larger than the reference temperature, which means that there is insufficient for the electrolyte to be replenished and the heat to be flushed away.

5. Conclusions

A multi-physics model is presented for numerical simulations of the generation and transfer of the heat. A simplified algorithm based on the Quasi Steady State ShortCut (QSSSC) is introduced to cheaply calculate the temperature evolution in QSS. The results in this work show that most of the reaction heat conducted into the electrodes during the pulse on-time and most of the joule heat is carried away by the electrolyte flow, which is due to that the electrolyte can't reach the turbulence state in near-wall area.

Acknowledgement

This work has been financially supported by the National Natural Science Foundation of China (No. 51576001), the Natural Science Foundation of Anhui Province of China (No. 1808085ME117) and the Scientific Research Foundation for the introduction of talents of Anhui Poly-technic University (No. 2018YQQ003).

References

- [1] Rajurkar K P, Sundaram M M and Malshe A P 2013 *Procedia CIRP* **6** 13-26
- [2] Rajurkar K P, Kozak J, Wei B and McGeough J A 1993 *CIRP Annals–Manufacturing Technology* **42** 231-234
- [3] Datta M and Landolt D 1981 *Electrochimica Acta* **26** 899-907
- [4] Kozak J, Rajurkar K P and Wei B 1994 *Journal of Engineering for Industry-Transactions of the ASME* **116** 316-323
- [5] Kozak J 2004 *Bulletin of the Polish Academy of Sciences: Technical Sciences* **52** 313–320
- [6] Kozak J 2013 *Proc. of the World Congress on Engineering and Computer Science* **II** 23-25
- [7] Smets N, Van Damme S, De Wilde D, et al. 2007 *Journal of Applied Electrochemistry* **37** 315-324
- [8] Smets N, Van Damme S, De Wilde D, et al. 2007 *Journal of Applied Electrochemistry* **37** 1345-1355
- [9] Smets N, Van Damme S, De Wilde D, et al. 2008 *Journal of Applied Electrochemistry* **38** 551-560
- [10] Smets N, Van Damme S, De Wilde D, et al. 2010 *Journal of Applied Electrochemistry* **40** 1395-1405
- [11] Deconinck D, Van Damme S, Albu C, et al. 2011 *Electrochimica Acta* **56** 5642-5649
- [12] Jaegle F, Cabrit O, Mendez S, et al. 2010 *Flow, Turbulence and Combustion* **85** 245-272
- [13] Deconinck D, Van Damme S and Deconinck J 2012 *Electrochimica Acta* **69** 120-127
- [14] Deconinck D, Hoogsteen W and Deconinck J 2013 *Electrochimica Acta* **103** 161-173